RSC Advances

PAPER

View Article Online
View Journal | View Issue



Cite this: *RSC Adv.*, 2024, **14**, 38944

# Preparation of a tetraethylenepentamine grafted magnetic chitosan bead for adsorption of Re(VII) from aqueous solutions

Chen Yang, [a] Xiaohui Wu[b] and Juan Mao[b]

A cross-linked magnetic chitosan bead (MCB) and tetraethylenepentamine grafted magnetic chitosan bead (TMCB) were synthesized using the water/oil (W/O) emulsion cross-linking method and characterized using scanning electron microscopy (SEM), vibrating-sample magnetometry (VSM) and Fourier transform infrared spectroscopy (FTIR). The saturation magnetization and remanent magnetization of TMCB were 7.09 emu $g^{-1}$ and 0.834 emu $g^{-1}$, respectively, illustrating the superparamagnetic properties of the prepared TMCB. The adsorption properties of MCB and TMCB for the removal of rare metal rhenium from acidic effluents were evaluated. Kinetic experimental data fit well with the pseudo-second-order model, and the adsorption isotherms were better fitted with the Langmuir model. The maximum adsorption capacities of Re(VII) as obtained from the Langmuir model were 224.50 and 257.61 mg $g^{-1}$ for MCB and TMCB, respectively, at pH 3 and 30 °C. Thermodynamic analysis revealed that the adsorption process is both spontaneous and exothermic. Regeneration experiments were conducted using 2 M NaCl, and TMCB maintained good adsorption and desorption performance after five regeneration cycles, indicating a promising material for the recovery of rhenium from acidic industrial effluents.

Received 15th August 2024
Accepted 13th November 2024

DOI: 10.1039/d4ra05927a

rsc.li/rsc-advances



## 1 Introduction

Rhenium is one of the rarest elements in the earth's crust. It plays an important role in various fields such as metallurgy, military, aviation, chemical and petrochemical industries owing to its high melting and boiling points and high hardness.[1] Although commercial rhenium is mainly extracted from molybdenum roaster-flue gas obtained from copper-sulfide ores, in many metallurgical enterprises in present China, rhenium still abundantly exists in the waste acid effluent produced from flue gas from non-ferrous metals smelting, which was directly discharged into wastewater treatment plant, reducing a waste of valuable resource. In recent years, the price of rhenium has risen rapidly as the demand for rhenium is growing quickly; thus, the recovery of Re(VII) from aqueous solutions is of great significance.[2]

Several methods for the recovery of rhenium, such as precipitation,[3] adsorption,[4] ion exchange[1] and solvent extraction,[5] have been widely used. Adsorption, with its advantages of environment-friendliness and high efficiency, has become a popular method for the removal of pollutants from wastewater. Compared to some expensive sorbents such as activated carbon and commercial chelating resins, biopolymers are considered a relatively low-cost alternative and are attracting increasing attention nowadays.[6]

Chitosan, a biopolymer obtained *via* the alkaline deacetylation of chitin, is a major component of crustaceans and one of the most abundant sorbents in nature.[7,8] As seen from recently reported literature, a great variety of precious metals were recovered using chitosan and/or its derivatives.[9,10] However, its drawbacks, such as weak mechanical properties, dissolution in acidic solution, low surface area, and separation difficulty, have hindered its applications for large-scale treatment of waste water.[11] Crosslinked chitosan with epichlorohydrin[6] or glutaraldehyde[12] has been proposed to improve its chemical stability and mechanical resistance. The crosslinking step may cause a decrease in metal uptake efficiency, especially when the chemical reactions involve amine groups.[13] Thus, crosslinked chitosan has been granulated in various forms with surface modification to introduce amine[14] and other functional groups.[15–17] These surface modification chitosan sorbents were with high selectivity, good acid resistance and sorption performance after modification. Moreover, as reported in literature,[18–20] techniques employing magnetism seem to be a good choice to solve the separation problem.

In the present work, tetraethylenepentamine-grafted magnetic chitosan bead (TMCB) with glutaraldehyde crosslinking was prepared to promote the adsorption performance of Re(VII) in an acidic solution. The characteristics of TMCB were confirmed through SEM, VSM and FTIR spectroscopy. Various factors affecting the uptake behavior such as pH value, contact time and temperature were investigated at the same time.

[a]*Department of Road and Rail, Hubei Communications Technical College, Wuhan, 430202, China*
[b]*School of Environmental Science and Engineering, Huazhong University of Science and Technology, Wuhan, 430074, China*

# 2 Materials and methods

## 2.1 Materials

Chitosan (90% acetylation degree), ferric chloride, ferrous sulfate, glutaraldehyde, epichlorohydrin, and tetraethylenepentamine were supplied by Sinopharm Chemical Reagent Co., Ltd (Shanghai, China). Re(VII) standard solution and potassium perrhenate were obtained from Sigma-Aldrich Co., Ltd (St. Louis, USA). All chemicals were reagent grade or above and used without further purification. All water mentioned in this work was doubly deionized water.

## 2.2 Preparation of sorbents

**2.2.1 Preparation of magnetic chitosan bead (MCB).** Magnetite supporting material was prepared using the modified Massart method.[21] A 250 mL $FeCl_3$ solution (0.2 M) was mixed with a 250 mL $FeSO_4$ solution (0.1 M), then a 200 mL ammonium hydroxide solution was poured into the above solution with vigorous stirring until a black precipitate was formed. The precipitate formed as ferroferric oxide microspheres was separated through magnetic decantation and washed with deionized water until the pH value decreases below 7.5 and dried in an oven at 60 °C.

Magnetic chitosan beads were prepared using the water/oil (W/O) emulsion cross-linking method.[22] 1 g of chitosan was dissolved in 20 mL of (2% v/v) acetic acid solution. Then, 0.35 g of magnetite was added into the chitosan solution, suspending with sonication for 30 min. The resulting solution was dropwise added into the oil phase, which consisted of 55 mL cyclohexane, 30 mL *n*-hexanol and 2 mL Span-80 as an emulsifier. The W/O emulsion system was agitated at room temperature (25 ± 2 °C) until microspheres were formed. Note that 1 mL of (25%, v/v) glutaraldehyde was dropped into the emulsion system, maintaining stirring for 2 h. The cross-linked microspheres were magnetically separated and rinsed with deionized water and ethanol several times and kept in a desiccator after drying at 60 °C.

**2.2.2 Preparation of tetraethylenepentamine grafted magnetic chitosan bead (TMCB).** Note that 3 mL of epichlorohydrin was dissolved in 20 mL acetone/water (1 : 1 v/v) solution, and then the wet magnetic chitosan bead obtained from above steps was added, with stirring for 12 h at 50 °C. The solid product was magnetically separated and washed using deionized water, followed by ethanol.

Then, epichlorohydrin-treated MCB was suspended in 20 mL of ethanol/water (1 : 1 v/v) solution, followed by adding 3 mL of tetraethylenepentamine for surface grafting. The suspension was agitated for 12 h at 50 °C, then tetraethylenepentamine-grafted MCB was magnetically separated and washed with deionized water and ethanol several times and kept in a desiccator for further adsorption experiments after drying at 60 °C. Schematic diagram of the preparation process of TMCB and the adsorption process of Re(VII) by TMCB are shown in Scheme 1.

## 2.3 Characteristic analysis methods

The surface morphologies of MCB and TMCB were examined with scanning electron microscopy (SEM, Nova NanoSEM 450 electron microscopy, FEI, Netherlands). A vibrating-sample magnetometer (VSM), provided by Physical Property Measurement System (Quantum Design Inc., San Diego, USA), was used to characterize the magnetic properties of $Fe_3O_4$ and TMCB at room temperature. Fourier transform infrared spectroscopy (FTIR) was used to compare the change of the functional groups in the ferroferric oxide microsphere, chitosan, TMCB, and Re(VII)-loaded TMCB. The infrared spectra of samples prepared as KBr discs were recorded by FTIR (VERTEX 70, Bruker Optics, German) within the range of 4000–400 $cm^{-1}$.

## 2.4 Batch experiments

**2.4.1 Effect of pH.** Note that 0.03 g of MCB or TMCB was added to 30 mL of 125 mg per L Re(VII) aqueous solution and agitated in a rotary shaker for 4 h at 140 rpm and 30 °C. The desired pH was adjusted using 1 M HCl or 1 M NaOH and measured with a pH meter (Starter 3C, OHAUS, USA). The residual concentration of Re(VII) as perrhenate anions ($ReO_4^-$) was determined using a UV-vis spectrometer (UV-260, Shimadzu, Japan) at 440 nm, followed by the method reported by D. Jermakowicz-Bartkowiak.[23] The amount of Re(VII) adsorbed per unit mass of adsorbent was calculated from the following equation:

$$q_e = \frac{C_i V_i - C_f V_f}{m} \quad (1)$$

where $V_i$ (mL) is the initial volume and $V_f$ (mL) is the final (initial plus added HCl or NaOH solution) volume. $C_i$ and $C_f$ (mg $L^{-1}$) are the initial and final Re(VII) concentrations, respectively, and $m$ (g) is the mass of biomass used.

**2.4.2 Adsorption kinetics.** Note that 1 g per L dosage of MCB or TMCB was contacted with 100 mL of 125 mg per L Re(VII) aqueous solution at pH 3 and 30 °C. Samples were collected at different time intervals (1, 3, 5, 7, 10, 20, 40, 60, 100, 180, 300 min) for the analysis of residual metal concentration in supernatant.

**2.4.3 Adsorption isotherms.** Isotherm studies were conducted by contacting 0.03 g of MCB or TMCB with 30 mL of Re(VII) solution at different initial concentrations ranging from 0 to 250 mg $L^{-1}$ at pH 3 for 24 h with a constant agitation speed of 140 rpm, under different temperatures at 30 °C, 40 °C and 50 °C, respectively. As soon as the equilibrium was attained, the residual concentration of Re(VII) was determined, followed by the method mentioned above.

## 2.5 Desorption and regeneration

In this study, eluents such as HCl, NaOH, and NaCl were chosen to regenerate the exhausted TMCB, which were exposed to 0.02 g of sorbent to 200 mg per L Re(II) solution at pH 3 and 30 °C for 24 h. The Re(VII)-loaded TMCB was collected and washed with deionized water for desorption. The Re(VII)-loaded TMCB were then immersed in 25 mL of 2 M NaCl solution for another 24 h. The remaining procedure was the same as mentioned above. The adsorption/desorption cycles were repeated five times for evaluating the sorbent performance.

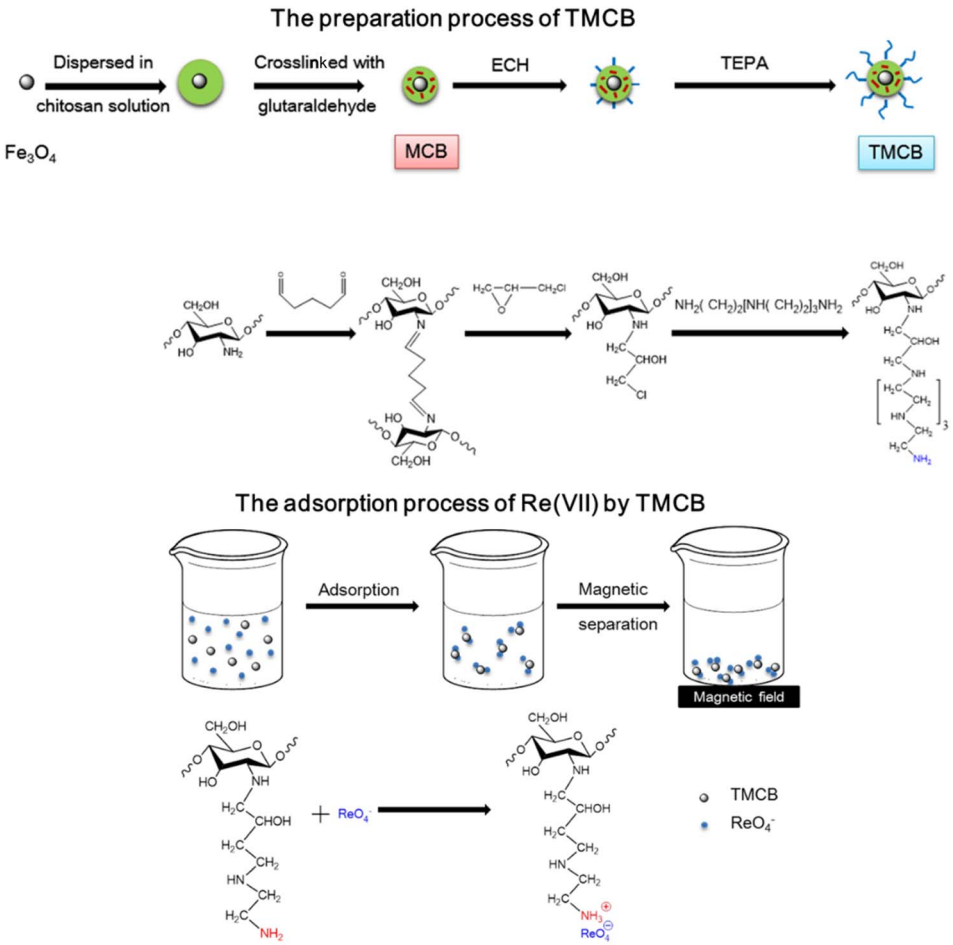


Scheme 1 Schematics of the preparation process of the TMCB and the adsorption process of Re(VII) by the TMCB.

# 3 Results and discussion

## 3.1 Characteristics of the sorbents

SEM analysis can provide information about the size and the surface morphology of the developed sorbents. As seen from Fig. 1a, the MCB exists as a core–shell with a diameter about 100 μm while TMCB shows a mean diameter of around 200 μm (Fig. 1b). Moreover, the surface of TMCB is more irregular and rougher than that of MCB, which indicates that tetraethylenepentamine seems to be successfully coated onto the surface of magnetic chitosan bead.

The magnetic property was measured on a vibrating sample magnetometer (VSM) and presented *via* the VSM plot of $H$ (Oe) and $M$ (emu $g^{-1}$). As shown in Fig. 1c, the saturation magnetization of TMCB and $Fe_3O_4$ are 7.09 emu $g^{-1}$ and 53.19 emu $g^{-1}$, respectively. The saturation magnetization of $Fe_3O_4$ decreased after modification may be attributed to chitosan coating on the surface of $Fe_3O_4$ and the relatively low amount of $Fe_3O_4$ loaded on the TMCB. However, the magnetic property remained high enough to meet the need for magnetic separation.[24]

The FTIR spectra of $Fe_3O_4$, TMCB, and Re(VII)-loaded TMCB are shown in Fig. 1d. For $Fe_3O_4$, a characteristic adsorption band at 588 $cm^{-1}$ is attributed to the stretching vibration of the Fe–O bond.[25] For chitosan, the adsorption band at around 3454 $cm^{-1}$ was assigned to the stretching vibration of O–H and N–H, and peaks at 2921 and 2876 $cm^{-1}$ are from the stretching vibrations of C–H bond; while adsorption peaks at around 1657, 1603 and 1383 $cm^{-1}$ can be attributed to amide band I, amide band II and $CH_3$ symmetrical angular deformation, respectively.[22] The IR spectra of TMCB contained the characteristic peaks of both chitosan and $Fe_3O_4$, which confirmed the successful coating of chitosan on $Fe_3O_4$ magnetic particles. For Re(VII)-loaded TMCB, a new peak at 914 $cm^{-1}$ is attributed to the Re=O bonds, suggesting that Re(VII) was successfully adsorbed by TMCB.[10]

## 3.2 Effect of pH

The effect of pH value of the medium on the uptake of Re(VII) is shown in Fig. 2. The sorption capacity of Re(VII) increased from 36 mg $g^{-1}$ to 88 mg $g^{-1}$ and 58 mg $g^{-1}$ to 103 mg $g^{-1}$ for MCB and TMCB, respectively, with pH value decreasing from 6 to 3. It can be concluded that the number of protonated amino groups was enhanced with lower pH conditions. Hence the more positively charged amine groups could electrostatically interact with negatively charged perrhenate ($ReO_4^-$). However, the uptake of Re(VII) decreased drastically for both MCB and TMCB

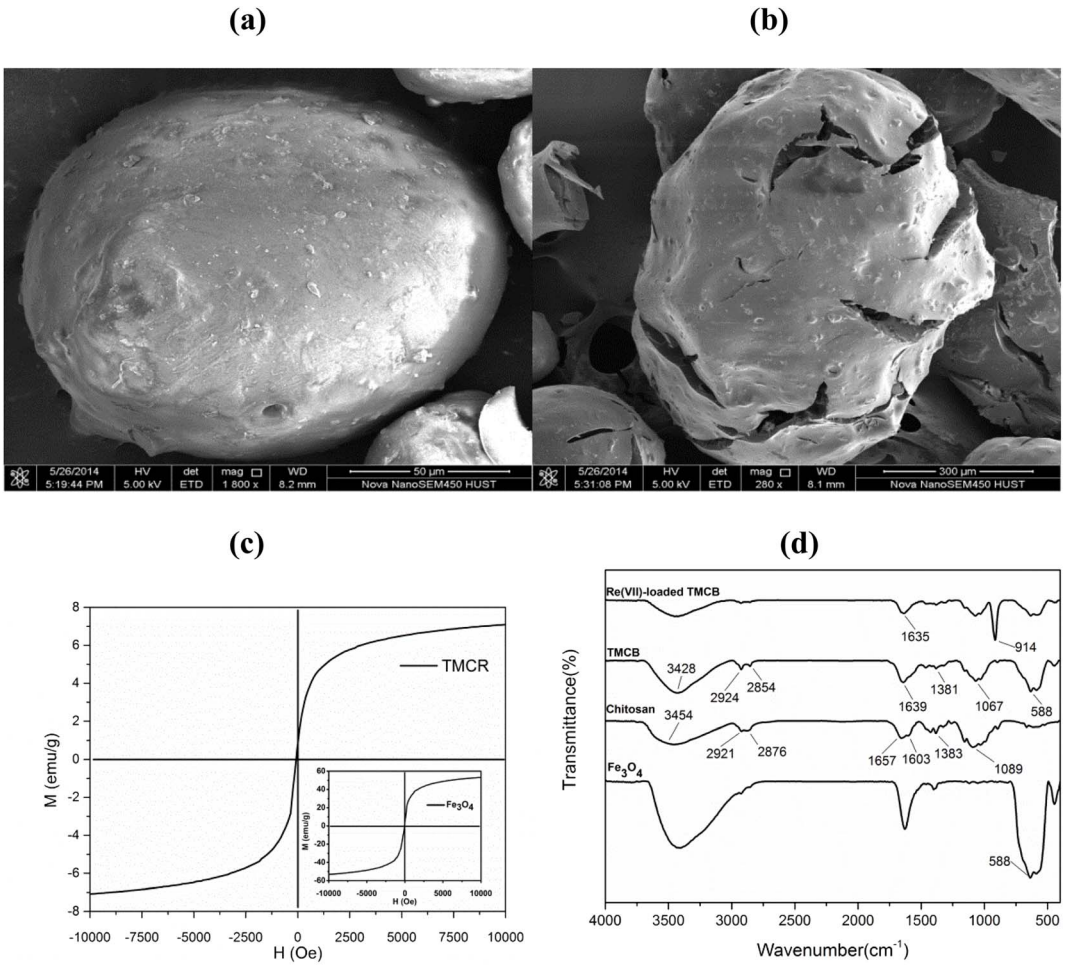


Fig. 1 SEM images of MCB (1800×) (a) and TMCB (280×) (b); VSM magnetization curves of TMCB and $Fe_3O_4$ (c); FTIR spectra of $Fe_3O_4$, chitosan, TMCB and Re(VII)-loaded TMCB (d).

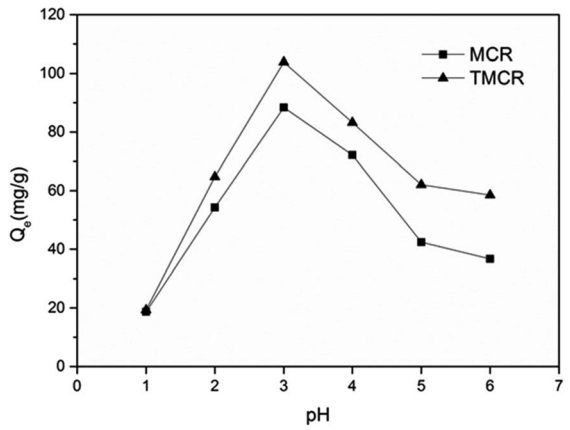


Fig. 2 Effect of pH on the uptake of Re(VII) ions by the MCB and TMCB.

as pH values reduced from 3 to 1, which can be attributed to a great deal of chloride anions at extremely low pH conditions which would interfere the adsorption of perrhenate anion ($ReO_4^-$) in the diffuse layer around the adsorbent by occupying the sites of protonated amine groups.[26]

### 3.3 Kinetic studies

Sorption kinetic study plays an important role in the treatment of aqueous effluents since it provides valuable information on the reaction pathway and in the mechanism of adsorption reactions. As shown in Fig. 3a, the adsorption equilibrium was reached within approximately 40 min for TMCB, whereas MCB took almost 100 min to attain equilibrium. A faster equilibrium time for TMCB was probably due to much more binding site ($-NH_3^+$) on the surface of sorbent after tetraethylenepentamine grafting, along with higher anionic $ReO_4^-$ favor. In order to investigate the adsorption kinetics mechanism of the sorbents for Re(VII), the pseudo-first-order model and pseudo-second-order model were introduced as follows:

Pseudo-first-order model:[27]

$$\ln(q_e - q_t) = \ln q_e - k_1 t \quad (2)$$

Pseudo-second-order model:[28]

$$\frac{t}{q_t} = \frac{1}{k_2 q_e^2} + \frac{t}{q_e} \quad (3)$$

where $k_1$ ($min^{-1}$) and $k_2$ ($g\ mg^{-1}\ min^{-1}$) are the rate constant of pseudo-first order model and pseudo-second-order model,

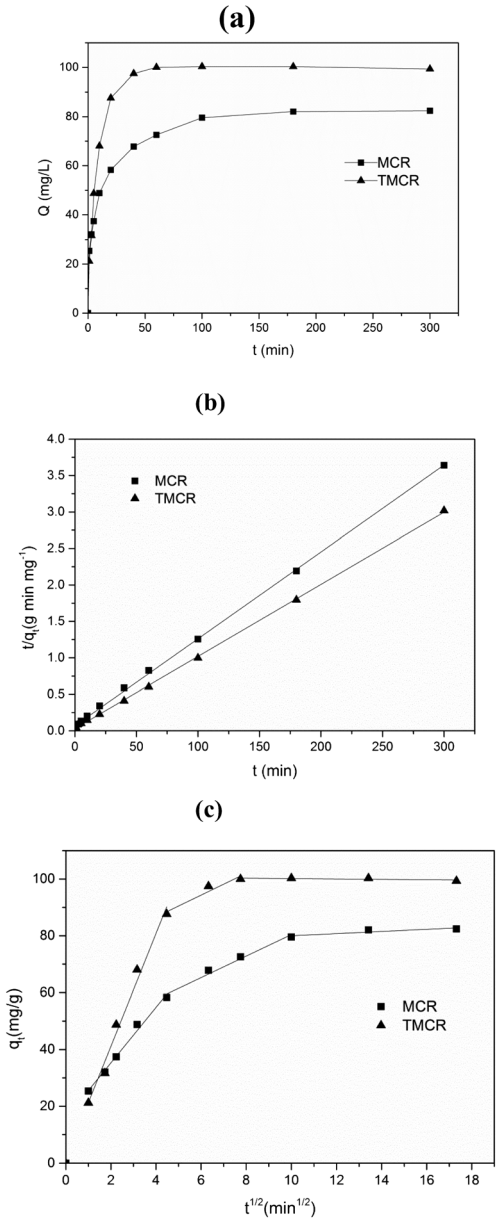


Fig. 3 (a) Effect of the contact time of Re(VII) adsorption by the MCB and TMCB at pH 3; (b) linearized pseudo-second-order kinetics model for the adsorption of Re(VII) onto MCB and TMCB; (c) intra-particle diffusion kinetics model for the adsorption of Re(VII) onto the MCB and TMCB.

respectively, $q_e$ and $q_t$ (mg g$^{-1}$) are the amounts of metal ions adsorbed on the adsorbents at equilibrium and at time $t$ (min), respectively.

The kinetic parameters obtained from the pseudo-first-order and pseudo-second-order models are summarized in Table 1 and the linearized form of the pseudo-second order model is given in Fig. 3b. As seen from Table 1, pseudo-second-order model fits the experimental data better than pseudo-first-order model, with higher correlation coefficient $R^2$ of 0.999. In addition, the calculated $q_e$ value obtained from pseudo-second-order model agreed well with experimental data. It implied that the rate-limiting step might be chemical sorption involving valency forces through sharing or electrons exchange between metal anions and chitosan bead.[28]

The relationship between the uptake and the root of time is used to determine the controlling step in the adsorption. The linear form of intra-particle diffusion equation can be described as below:[29]

$$q_t = K_{id} t^{0.5} \quad (4)$$

where $K_{id}$ is the intraparticle diffusion rate (mg g$^{-1}$ min$^{-0.5}$). Fig. 3c shows the intra-particle diffusion plots for Re(VII) adsorption on both MCB and TMCB, dividing into three stages.[25] The diffusion rate constants in every step are depicted in Table 1. In the first step, large numbers of Re(VII) anion were adsorbed instantly by the external surface of sorbents. In the second step, the Re(VII) anion gradually entered into the interior pores of sorbents and adsorbed into the interior surface until the adsorption equilibrium was reached. In the third step, as seen in Table 1, the intra-particle diffusion rate constant $K_{i3}$ was about zero, indicating that the final equilibrium state was reached. The much higher $K_{i1}$ and $K_{i2}$ values for TMCB than that for MCB might be attributed to more active sites on the external or interior surface of TMCR. Besides, straight lines of the beginning period did not pass through the origin, suggesting that intraparticle diffusion was not the rate-limiting step for the whole reaction.[30]

### 3.4 Adsorption isotherms

Isotherms are used to describe the maximal adsorption capacity of the adsorbent and reveal the adsorption behaviors between adsorbate and adsorbent. As shown in Fig. 4, the uptake of Re(VII) onto TMCB increased with increasing equilibrium concentration under different temperature ranging from 30 °C to 50 °C.

The adsorption isotherm data was treated according to Langmuir[31] and Freundlich[32] models:

$$\frac{C_e}{q_e} = \frac{C_e}{q_m} + \frac{1}{q_m K_L} \quad (5)$$

Table 1 Pseudo-first-order and pseudo-second-order parameters of Re(VII) adsorption on the MCB and TMCB

| | Pseudo-first-order | | | Pseudo-second-order | | | Intra-particle diffusion model | | |
|---|---|---|---|---|---|---|---|---|---|
| Adsorbent | $k_1$ (min$^{-1}$) | $q_e$ (mg g$^{-1}$) | $R^2$ | $k_2$ (g mg$^{-1}$ min$^{-1}$) | $q_e$ (mg g$^{-1}$) | $R^2$ | $k_{i1}$ | $k_{i2}$ (mg g$^{-1}$ min$^{-1/2}$) | $k_{i3}$ |
| MCB | 0.053 | 33.540 | 0.954 | 0.002073 | 84.03 | 0.999 | 12.41 | 3.79 | 0 |
| TMCB | 0.0127 | 4.712 | 0.976 | 0.003267 | 101.01 | 0.999 | 20.09 | 3.85 | 0 |

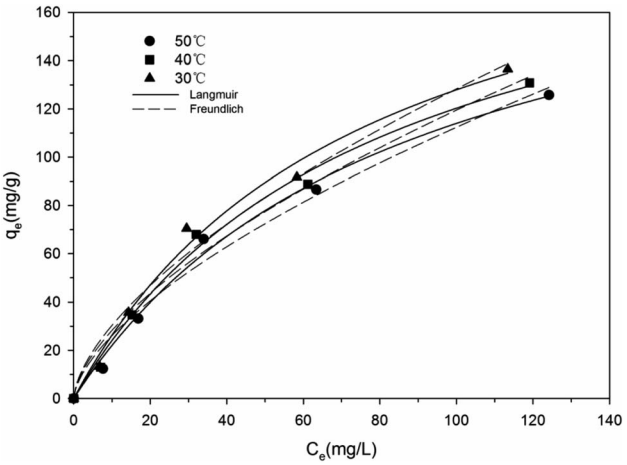


Fig. 4 Isotherms of Re(VII) adsorption by the MCB and TMCB at different temperatures (30 °C, 40 °C and 50 °C). The isotherm experimental data were described using the Langmuir (solid line) and Freundlich (dashed line) models.

$$q_e = K_f C_e^{1/n} \quad (6)$$

where $q_e$ (mg $g^{-1}$) is the amount of Re(VII) adsorbed per MCB or TMCB at equilibrium, and $C_e$ (mg $L^{-1}$) is the equilibrium Re(VII) concentration remaining in the solution, $q_m$ (mg $g^{-1}$) is the maximum adsorption capacity of Re(VII) and, $K_L$ (L $mg^{-1}$) is the Langmuir equilibrium constant which is related to the free energy of adsorption, $K_f$ is the Freundlich constant relating the adsorption capacity, and $n$ is the Freundlich exponent.

The Langmuir and Freundlich equation parameters, calculated from their respective isotherms along with the coefficients of determination are presented in Table 2. As shown in Table 2, Langmuir isotherm model yielded higher value of correlation coefficients ($R^2$) compared to Freundlich isotherm model suggesting that the adsorption of Re(VII) onto the surfaces of MCB and TMCB follows a monolayer coverage involving chemisorption.[16] According to the Langmuir isotherm model, the theoretical maximum Re(VII) adsorption capacities of TMCB under different temperatures (30 °C, 40 °C and 50 °C) were obtained as 257.61, 255.01 and 249.24 mg $g^{-1}$, respectively, higher than those of MCR (224.50, 216.5, 212.78 mg $g^{-1}$); also, the $K_L$ of TMCB observed under different temperatures were 0.0188, 0.0143 and 0.0116 L $mg^{-1}$, respectively, higher than that of MCB (0.0133, 0.0125 and 0.0115 L $mg^{-1}$). This indicated that TMCB possessed more amino binding sites than MCB, and took advantage of the electrostatic adsorption of Re(VII). Likewise, the $n$ values calculated from the Freundlich isotherm equation were between 1.59 and 1.66 for both MCB and TMCB, reflecting that the adsorption process was favorable.[33] Comparing the sorption capacity of rhenium reported in the literature,[4,23,34] both MCB and TMCB prevailed over all reported sorbents.

It was observable that the adsorption capacity of Re(VII) decreased with increasing temperature from 30 °C to 50 °C, indicating that the adsorption reaction is exothermic. Thermodynamic parameters of adsorption were calculated from the following van't Hoff equation:[35]

$$\ln K_L = -\frac{\Delta H^\circ}{RT} + \frac{\Delta S^\circ}{R} \quad (7)$$

where $\Delta H^\circ$ (J $mol^{-1}$) and $\Delta S^\circ$ (J $mol^{-1}$ $K^{-1}$) are enthalpy and entropy changes, $R$ is the universal gas constant (8.314 J $mol^{-1}$ $K^{-1}$) and $T$ is the absolute temperature (K). Plotting $\ln K_L$ against $1/T$ gives a straight line with slope and intercept equal to $-\Delta H^\circ/R$ and $\Delta S^\circ/R$, respectively. The values of $\Delta H^\circ$ and $\Delta S^\circ$ were calculated as −5.76 kJ $mol^{-1}$ and −11.46 J $mol^{-1}$ $K^{-1}$, respectively, for MCB; while higher values ($\Delta H^\circ$: −19.71 kJ $mol^{-1}$, $\Delta S^\circ$: −54.71 J $mol^{-1}$ $K^{-1}$) obtained from thermodynamic adsorption of TMCB. The negative value of $\Delta H^\circ$ indicates an exothermic adsorption process and the negative values of $\Delta S^\circ$ might be due to the high orderness of the adsorption system at equilibrium. Gibbs free energy of ($\Delta G^\circ$), the fundamental criterion of spontaneity, was calculated from the following relation:

$$\Delta G^\circ = \Delta H^\circ - T\Delta S^\circ \quad (8)$$

The negative value of $\Delta G^\circ$ indicates that the adsorption reaction is spontaneous. As seen in Table 2, $\Delta G^\circ$ is negative and increases with increasing temperature indicating that the adsorption of Re(VII) is spontaneous and, spontaneity decreases in higher temperatures, which is consistent with the results of isotherm that higher temperature resulting less favorable Re(VII) adsorption.[36]

### 3.5 Regeneration

Regeneration study is important to figure out the possibility for the recovery of metals adsorbed on the sorbent. In this study, 2 M NaCl was employed as eluents. The mechanism of

Table 2 Isotherm parameters for the adsorption of Re(VII) onto the MCB and TMCB at different temperatures

| | | Langmuir model | | | | Freundlich model | | |
|---|---|---|---|---|---|---|---|---|
| Adsorbent | Temp. (K) | $Q_{max}$ (mg $L^{-1}$) | $K_L$ (L $mg^{-1}$) | $R^2$ | $\Delta G^\circ$ (kJ $mol^{-1}$) | $K_F$ (mg $g^{-1}$) (dm$^3$ $g^{-1}$)$^{1/n}$ | $n$ | $R^2$ |
| MCB | 303 | 224.50 | 0.0133 | 0.991 | −3.13 | 7.182 | 1.597 | 0.949 |
| | 313 | 216.50 | 0.0125 | 0.997 | −2.59 | 6.684 | 1.597 | 0.955 |
| | 323 | 212.78 | 0.0115 | 0.993 | −2.04 | 6.074 | 1.578 | 0.954 |
| TMCB | 303 | 257.61 | 0.0188 | 0.994 | −2.29 | 11.25 | 1.66 | 0.971 |
| | 313 | 255.01 | 0.0143 | 0.990 | −2.17 | 8.95 | 1.62 | 0.982 |
| | 323 | 249.24 | 0.0116 | 0.993 | −2.06 | 7.42 | 1.59 | 0.994 |

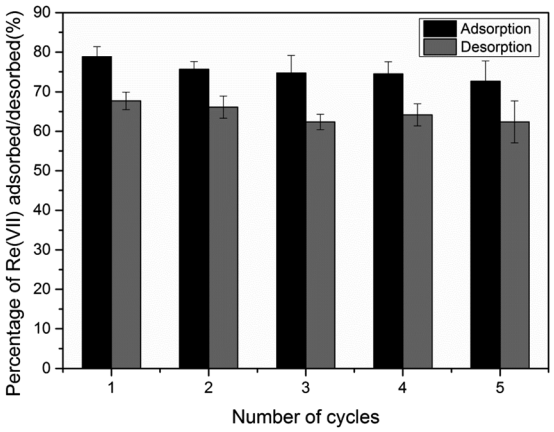


Fig. 5 Adsorption/desorption cycles for the TMCB.

desorption reaction might be due to the electrostatic interaction between Re(VII) oxoanion and the charged species in elution, through the compression of the electric double layer, which would weaken the interaction between adsorbent and metal, promoting desorption performance;[37] meanwhile, the negatively charged Re(VII) was replaced with chloride ion, which was contacted with positively charged amine groups on the surface of TMCB. The desorption reaction can be expressed as the following equation:

$$\text{TMCB–NH}_3^+\text{ReO}_4^- + \text{NaCl} = \text{TMCB–NH}_3^+\text{Cl}^- + \text{NaReO}_4$$

The adsorption/desorption cycles were repeated five times as shown in Fig. 5. The results show that both sorption and desorption efficiency capacity of TMCB are quite stable with over 72% of sorption efficiency and over 62% of desorption efficiency after the fifth cycle. This result showed a great potential for regeneration of exhausted TMCB in further application.

## 4 Conclusions

In this study, tetraethylenepentamine grafted magnetic chitosan bead was synthesized and characterized. SEM, VSM and FTIR analysis illuminated that chitosan was successfully coated on the surface of $Fe_3O_4$ particles. pH effect demonstrated that pH 3 was the best condition for Re(VII) adsorption. TMCB for Re(VII) adsorption equilibrium was rapidly achieved within 40 min, with kinetic data described well by the pseudo-second-order model, indicating a chemical adsorption is a rate-limiting step. Equilibrium isotherm data were fitted with Langmuir and Freundlich models, and the Langmuir model was in good agreement with the experimental data with a higher $R^2$. TMCB presented higher uptake capacity of Re(VII) (257.61 mg $L^{-1}$) compared to MCB with an uptake of 224.50 mg $L^{-1}$, which indicated the grafting of amine groups was accomplished. The thermodynamic parameters indicated an orderly, spontaneous and exothermic adsorption process. Also, TMCB can be easily regenerated only using 2 M NaCl, exhibiting quite a good desorption performance even after five adsorption–desorption cycles. Therefore, tetraethylenepentamine grafted magnetic chitosan bead can be a potential alternative absorbent for separating Re(VII) from aqueous solutions, with the advantage of easy magnetic separation, favorable kinetic characteristics and, high adsorption and desorption performance.

## Data availability

The authors declare that the data supporting the findings of this study are available within the paper.

## Conflicts of interest

There are no conflicts to declare.

## References

1 M. Jia, H. Cui, W. Jin, *et al.*, Adsorption and separation of rhenium(VII) using *N*-methylimidazolium functionalized strong basic anion exchange resin, *J. Chem. Technol. Biotechnol.*, 2013, **88**(3), 437–443, DOI: 10.1002/jctb.3904.
2 C. Xiong, C. Yao and X. Wu, Adsorption of rhenium(VII) on 4-amino-1,2,4-triazole resin, *Hydrometallurgy*, 2008, **90**, 221–226, DOI: 10.1016/j.hydromet.2007.10.011.
3 D. G. Petrov, I. D. Troshkina, A. M. Chekmarev, *et al.*, Precipitation recovery of rhenium(VII) from aqueous solutions with coagulating cationic polyelectrolyte, *Russ. J. Appl. Chem.*, 2001, **74**, 954–957, DOI: 10.1023/A:1013061321925.
4 S. Seo, W. S. Choi, T. J. Yang, *et al.*, Recovery of rhenium and molybdenum from a roaster fume scrubbing liquor by adsorption using activated carbon, *Hydrometallurgy*, 2012, **129**, 145–150, DOI: 10.1016/j.hydromet.2012.06.007.
5 C. Zhan-Fang, Z. Hong and Q. Zhao-Hui, Solvent extraction of rhenium from molybdenum in alkaline solution, *Hydrometallurgy*, 2009, **97**(3–4), 153–157, DOI: 10.1016/j.hydromet.2009.02.005.
6 W. S. W. Ngah, C. S. Endud and R. Mayanar, Removal of copper(II) ions from aqueous solution onto chitosan and cross-linked chitosan beads, *React. Funct. Polym.*, 2002, **50**(2), 181–190, DOI: 10.1016/S1381-5148(01)00113-4.
7 P. Methacanon, M. Prasitsilp, T. Pothsree, *et al.*, Heterogeneous *N*-deacetylation of squid chitin in alkaline solution, *Carbohydr. Polym.*, 2003, **52**(2), 119–123, DOI: 10.1016/S0144-8617(02)00300-4.
8 E. Guibal, Interactions of metal ions with chitosan-based sorbents: a review, *Sep. Purif. Technol.*, 2004, **38**(1), 43–74, DOI: 10.1016/j.seppur.2003.10.004.
9 E. Repo, R. Koivula, R. Harjula, *et al.*, Effect of EDTA and some other interfering species on the adsorption of Co(II) by EDTA-modified chitosan, *Desalination*, 2013, **321**, 93–102, DOI: 10.1016/j.desal.2013.02.028.
10 Y. Xiong, L. Xie, *et al.*, Superior adsorption of Re(VII) by anionic imprinted chitosan-silica composite: adsorption performance, selectivity and mechanism study, *J. Ind. Eng. Chem.*, 2022, **108**, 344–355, DOI: 10.1016/j.jiec.2022.01.013.

11 B. Alizadeh, M. Delnavaz and A. Shakeri, Removal of Cd(II) and phenol using novel cross-linked magnetic EDTA/chitosan/TiO$^2$ nanocomposite, *Carbohydr. Polym.*, 2018, **181**, 675–683, DOI: 10.1016/j.carbpol.2017.11.095.

12 R. S. Vieira and M. M. Beppu, Dynamic and static adsorption and desorption of Hg(II) ions on chitosan membranes and spheres, *Water Res.*, 2006, **40**(8), 1726–1734, DOI: 10.1016/j.watres.2006.02.027.

13 M. S. D. Erosa, T. I. S. Medina, R. N. Mendoza, *et al.*, Cadmium sorption on chitosan sorbents: kinetic and equilibrium studies, *Hydrometallurgy*, 2001, **61**(3), 157–167, DOI: 10.1016/S0304-386X(01)00166-9.

14 X. Hu, J. Wang, Y. Liu, *et al.*, Adsorption of chromium(VI) by ethylenediamine-modified cross-linked magnetic chitosan resin: isotherms, kinetics and thermodynamics, *J. Hazard. Mater.*, 2011, **185**(1), 306–314, DOI: 10.1016/j.jhazmat.2010.09.034.

15 M. Monier, D. M. Ayad and D. A. Abdel-Latif, Adsorption of Cu(II), Cd(II) and Ni(II) ions by cross-linked magnetic chitosan-2-aminopyridine glyoxal Schiff's base, *Colloids Surf., B*, 2012, **94**, 250–258, DOI: 10.1016/j.colsurfb.2012.01.051.

16 T. L. Lin and H. L. Lien, Effective and selective recovery of precious metals by thiourea modified magnetic nanoparticles, *Int. J. Mol. Sci.*, 2013, **14**(5), 9834–9847, DOI: 10.3390/ijms14059834.

17 A. H. Jawad, A. S. Abdulhameed, A. Hapiz, *et al.*, Fabrication of Magnetic Chitosan-Benzil Biopolymer with Organoclay for Remazol Brilliant Blue R Dye Removal: A Statistical Modeling and Adsorption Mechanism, *J. Inorg. Organomet. Polym. Mater.*, 2024, **34**, 4450–4462, DOI: 10.1007/s10904-024-03120-5.

18 M. Monier, D. M. Ayad, Y. Wei, *et al.*, Adsorption of Cu(II), Co(II), and Ni(II) ions by modified magnetic chitosan chelating resin, *J. Hazard. Mater.*, 2010, **177**(1–3), 962–970, DOI: 10.1016/j.jhazmat.2010.01.012.

19 Y. G. Zhao, H. Y. Shen, S. D. Pan, *et al.*, Synthesis, characterization and properties of ethylenediamine-functionalized $Fe_3O_4$ magnetic polymers for removal of Cr(VI) in wastewater, *J. Hazard. Mater.*, 2010, **182**(1–3), 295–302, DOI: 10.1016/j.jhazmat.2010.06.029.

20 X. An, Z. Su and H. Zeng, Preparation of highly magnetic chitosan particles and their use for affinity purification of enzymes, *J. Chem. Technol. Biotechnol.*, 2003, **78**(5), 596–600, DOI: 10.1002/jctb.820.

21 A. M. Donia, A. M. Yousif, A. A. Atia, *et al.*, Efficient adsorption of Ag(I) and Au(III) on modified magnetic chitosan with amine functionalities, *Desalin. Water Treat.*, 2014, **52**(13–15), 2537–2547, DOI: 10.1080/19443994.2013.794706.

22 M. Monier, D. M. Ayad, Y. Wei, *et al.*, Preparation and characterization of magnetic chelating resin based on chitosan for adsorption of Cu(II), Co(II), and Ni(II) ions, *React. Funct. Polym.*, 2010, **70**(4), 257–266, DOI: 10.1016/j.reactfunctpolym.2010.01.002.

23 D. Jermakowicz-Bartkowiak and B. N. Kolarz, Poly(4-vinylpyridine) resins towards perrhenate sorption and desorption, *React. Funct. Polym.*, 2011, **71**(2), 95–103, DOI: 10.1016/j.reactfunctpolym.2010.11.023.

24 N. A. Travlou, G. Z. Kyzas, N. K. Lazaridis, *et al.*, Functionalization of graphite oxide with magnetic chitosan for the preparation of a nanocomposite dye adsorbent, *Langmuir*, 2013, **29**(5), 1657–1668, DOI: 10.1021/la304696y.

25 Y. Ren, H. A. Abbood, F. He, *et al.*, Magnetic EDTA-modified chitosan/$SiO_2$/$Fe_3O_4$ adsorbent: preparation, characterization, and application in heavy metal adsorption, *Chem. Eng. J.*, 2013, **226**, 300–311, DOI: 10.1016/j.cej.2013.04.059.

26 E. Kim, M. F. Benedetti and J. Boulègue, Removal of dissolved rhenium by sorption onto organic polymers: study of rhenium as an analogue of radioactive technetium, *Water Res.*, 2004, **38**(2), 448–454, DOI: 10.1016/j.watres.2003.09.033.

27 L. Zhou, Z. Liu, J. Liu, *et al.*, Adsorption of Hg(II) from aqueous solution by ethylenediamine-modified magnetic crosslinking chitosan microspheres, *Desalination*, 2010, **258**(1–3), 41–47, DOI: 10.1016/j.desal.2010.03.051.

28 Y. S. Ho and G. McKay, Pseudo-second order model for sorption processes, *Process Biochem.*, 1999, **34**(5), 451–465, DOI: 10.1016/S0032-9592(98)00112-5.

29 S. K. Singh, T. G. Townsend, D. Mazyck, *et al.*, Equilibrium and intra-particle diffusion of stabilized landfill leachate onto micro-and meso-porous activated carbon, *Water Res.*, 2012, **46**(2), 491–499, DOI: 10.1016/j.watres.2011.11.007.

30 Y. S. Ho and A. E. Ofomaja, Kinetics and thermodynamics of lead ion sorption on palm kernel fibre from aqueous solution, *Process Biochem.*, 2005, **40**(11), 3455–3461, DOI: 10.1016/j.procbio.2005.02.017.

31 I. Langmuir, The adsorption of gases on plane surfaces of glass, mica and platinum, *J. Am. Chem. Soc.*, 1918, **40**(9), 1361–1403, DOI: 10.1021/ja02242a004.

32 H. Freundlich, Über die adsorption in lösungen, *Z. Phys. Chem.*, 1907, **57**(1), 385–470, DOI: 10.1515/zpch-1907-5723.

33 S. Changmei, Z. Guanghua, W. Chunhua, *et al.*, A resin with high adsorption selectivity for Au(III): preparation, characterization and adsorption properties, *Chem. Eng. J.*, 2011, **172**(2–3), 713–720, DOI: 10.1016/j.cej.2011.06.040.

34 A. V. Plevaka, I. D. Troshkina, L. A. Zemskova, *et al.*, Rhenium sorption by fibrous chitosan-carbon materials, *Russ. J. Inorg. Chem.*, 2009, **54**, 1168–1171, DOI: 10.1134/S0036023609070286.

35 J. Tellinghuisen, Van't Hoff analysis of $K°(T)$: how good… or bad?, *Biophys. Chem.*, 2006, **120**(2), 114–120, DOI: 10.1016/j.bpc.2005.10.012.

36 A. M. Donia, A. A. Atia and K. Z. Elwakeel, Recovery of gold(III) and silver(I) on a chemically modified chitosan with magnetic properties, *Hydrometallurgy*, 2007, **87**(3–4), 197–206, DOI: 10.1016/j.hydromet.2007.03.007.

37 P. Baroni, R. S. Vieira, E. Meneghetti, *et al.*, Evaluation of batch adsorption of chromium ions on natural and crosslinked chitosan membranes, *J. Hazard. Mater.*, 2008, **152**(3), 1155–1163, DOI: 10.1016/j.jhazmat.2007.07.099.